Available online at www.sciencedirect.com
SCIENCE DIRECT®
Journal of Organometallic Chemistry 680 (2003) 182–187
Journal of Organometallic Chemistry
www.elsevier.com/locate/jorganchem

9-BBN activation. Synthesis, crystal structure and theoretical characterization of the ruthenium complex $Ru[(\mu\text{-}H)_2BC_8H_{14}]_2(PCy_3)$

Khaled Essalah [a,1], Jean-Claude Barthelat [a], Virginia Montiel [b], Sébastien Lachaize [b], Bruno Donnadieu [b], Bruno Chaudret [b], Sylviane Sabo-Etienne [b,*]

[a] Laboratoire de Physique Quantique, IRSAMC (UMR 5626), Université Paul Sabatier, 118 route de Narbonne, 31062 Toulouse Cedex 4, France
[b] Laboratoire de Chimie de Coordination du CNRS, 205 route de Narbonne, 31077 Toulouse Cedex 4, France

Received 21 March 2003; received in revised form 23 April 2003; accepted 23 April 2003

Abstract

Reaction of the bis(dihydrogen) ruthenium complex $RuH_2(H_2)_2(PCy_3)_2$ (**1**) with an excess of 9-borabicyclononane yields $Ru[(\mu\text{-}H)_2BC_8H_{14}]_2(PCy_3)$ (**6**) and the phosphine adduct $PCy_3 \cdot HBC_8H_{14}$. The new complex is characterized by NMR spectroscopy and X-ray diffraction. New X-ray data on 9-BBN dimer, from a measurement at 180 K, are also reported. DFT calculations (B3LYP) on $Ru[(\mu\text{-}H)_2BC_8H_{14}]_2(PMe_3)$ (**7**), the PMe_3 analogue of **6**, confirm the ruthenium (II) formulation with two dihydroborate ligands. The data obtained using PH_3 or PMe_3 as models for PCy_3 in $PR_3 \cdot HBC_8H_{14}$ are also discussed.

Keywords: Boranes; Ruthenium; Polyhydrides; DFT; 9-BBN

1. Introduction

Borane activation by transition metal complexes continues to attract considerable attention, not only because of the catalytic potential but also because of the versatile structures and bonding modes associated to this chemistry. The last decade has shown considerable achievement on the characterization of boryl and σ-borane complexes and on the involvement of these species in several catalytic processes such as hydroboration or diboration of unsaturated substrates, and functionalization of alkanes and arenes [1–7].

Our group is currently involved in investigations based on the activation of boranes by the ruthenium bis(dihydrogen) precursor $RuH_2(H_2)_2(PCy_3)_2$ (**1**) [8]. Our first results show that the nature of the final product is highly dependent on the experimental conditions (stoichiometric ratio, solvent...) and on the nature of the boron reagent. In particular, we have recently shown that σ-complexes can be stabilized by using the tricoordinated neutral pinacolborane compound [9]. The complex $RuH[(\mu\text{-}H)_2Bpin](\sigma\text{-}HBpin)(PCy_3)_2$ (**2**) ($HBpin = HBO_2C_2Me_4$) can thus be synthesized by adding an excess of HBpin to **1**. The two boron ligands are attached to the ruthenium center by two different coordination modes: σ-coordination and dihydroborate ligation. When using only one equivalent HBpin, the complex $RuH_2(\sigma\text{-}H_2)(\sigma\text{-}HBpin)(PCy_3)_2$ (**3**) can be generated. X-ray data and theoretical calculations demonstrate that **3** is stabilized by two σ-ligands, a borane and a dihydrogen [10]. In the case of 9-borabicyclononane (9-BBN dimer = $(HBC_8H_{14})_2$) activation, we reported some years ago that addition of one equivalent of 9-BBN to a suspension of **1** in hexane led to the formation of a dihydroborate compound $RuH[(\mu\text{-}H)_2B\text{-}C_8H_{14}](PCy_3)_2$ (**4**) characterized by NMR data as a 16 electron complex [11]. Dihydrogen bubbling led to borane elimination and regeneration of the starting complex **1** via the dihydrogen intermediate $RuH[(\mu\text{-}H)_2\ BC_8H_{14}](H_2)(PCy_3)_2$ (**5**).

We now describe the synthesis and characterization of a new ruthenium complex $Ru[(\mu\text{-}H)_2BC_8H_{14}]_2(PCy_3)$ (**6**) resulting also from the activation of 9-borabicyclono-

* Corresponding author. Tel.: +33-5-61-333177; fax: +33-5-61-553003.
E-mail address: sabo@lcc-toulouse.fr (S. Sabo-Etienne).
[1] Permanent address: Unité de Recherche de Physico-Chimie Moléculaire, Institut Préparatoire des Etudes Scientifiques et Techniques (IPEST), Boite Postale 51, 2070 La Marsa, Tunisia.

0022-328X/03/$ - see front matter
doi:10.1016/S0022-328X(03)00343-7

nane. X-ray data and theoretical calculations support the formulation of a bis(dihydroborate) complex.

2. Results and discussion

Addition of an excess of 9-BBN dimer to a toluene suspension of $RuH_2(H_2)_2(PCy_3)_2$ (**1**) results in gas evolution and formation of an orange solution. Cooling at −35 °C affords an orange solid analyzed as $Ru[(\mu\text{-}H)_2BC_8H_{14}]_2(PCy_3)$ (**6**) (see Scheme 1) and characterized by NMR and X-ray diffraction. The ^{1}H-NMR spectrum of **6** shows one broad high field resonance at room temperature at δ −12.34 resolved as a doublet between 263 and 233 K indicative of a coupling with only one phosphine with a J_{H-P} constant of 9 Hz. The relaxation time T_1 of the hydrides has been determined as 95 ms at 243 K and 300 MHz in agreement with the absence of any dihydrogen ligand. The presence of four hydrides is confirmed by the observation of a quintet at δ 104.9 ($J_{H-P} = 9$ Hz) on the ^{31}P-NMR spectrum recorded with selective decoupling of the protons of the PCy_3 ligand. The ^{11}B-NMR spectrum of **6** shows one broad resonance at room temperature at δ 58.8. Similar chemical shifts were reported for dihydroborate niobocene complexes [12,13].

The X-ray structure determined at 160 K is depicted in Fig. 1. Crystal data are reported in Table 1 and selected bond distances and angles are listed in Table 2 together with DFT results for comparison (see below). The ruthenium is surrounded by one phosphine and two dihydroborate ligands with a B1–Ru–B2 angle of 147.68(8)°. The Ru–P distance is 2.2150(5) Å. As a result of a vacancy *trans* to the phosphine, this value is shorter than what is normally found for other ruthenium complexes with PCy_3 ligand (ca. 2.35 Å) [8,9,14]. The two P–Ru–B angles are slightly different and equal to 103.89(6) and 108.37(6)°. The Ru–B1 distance is

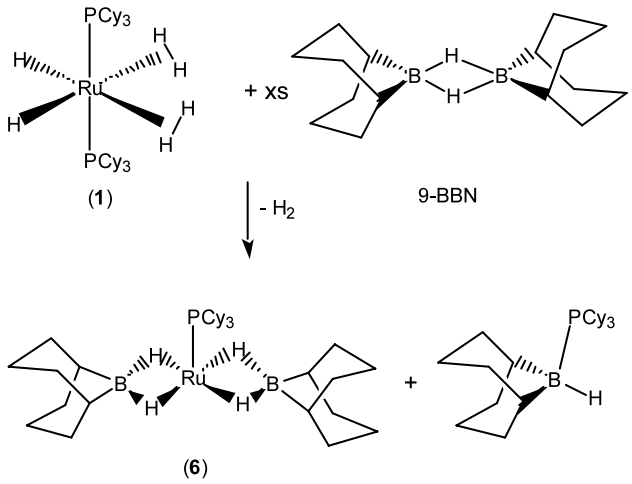

Scheme 1.

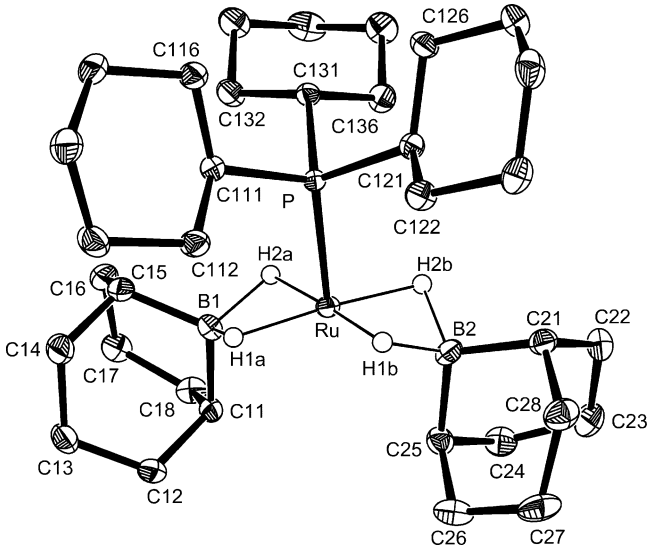

Fig. 1. ORTEP drawing of complex $Ru[(\mu\text{-}H)_2BC_8H_{14}]_2(PCy_3)$ (**6**).

Table 1
Crystal data for $Ru[(\mu\text{-}H)_2BC_8H_{14}]_2(PCy_3)$ (**6**)

Chemical formula	$C_{34}H_{65}B_2PRu$
Formula weight	627.52
Crystal system	triclinic
Space group	$P\bar{1}$
Z, calculated density (Mg m^{-3})	2, 1.273
Absorption coefficient (mm^{-1})	0.549
$F(0\,0\,0)$	676
a (Å)	10.4997(12)
b (Å)	11.0584(12)
c (Å)	15.6545(18)
α (°)	77.927(13)
β (°)	80.427(13)
γ (°)	67.742(12)
V (Å)	1637.4(3)
Temperature (K)	160(2)
Data/restraints/parameters	5959/0/359
Goodness of fit on F^2	1.041
$R_1[I > 2\sigma(I)]$	0.0233
wR_2	0.0570
Largest difference peak and hole (e Å^{-3})	0.405 and −0.451

2.160(2) Å, whereas the Ru–B2 distance is 2.085(2) Å, thus slightly shorter. Analysis of the distances involving the hydrogen atoms bound to the ruthenium should be considered cautiously. Four hydrogen atoms were however located in the vicinity of the ruthenium with Ru–H distances of 1.63 Å (av). The ruthenium and the four hydrogen atoms H(1a), H(1b), H(2a) and H(2b) are coplanar. The distances between the two borons and the hydrogens are in the range 1.35(2) and 1.41(2) Å. These values are close to those found in niobium metal complexes coordinating the 9-BBN ligand in a similar fashion. The B–H distances in $Cp_2Nb[(\mu\text{-}H)_2BC_8H_{14}]$ are 1.38(7) and 1.39(6) Å [12], whereas slightly different values were obtained for the substituted $SiMe_3C_5H_4$

Table 2
X-ray data for $Ru[(\mu\text{-}H)_2BC_8H_{14}]_2(PCy_3)$ (**6**) and selected B3LYP-optimized geometrical parameters for $Ru[(\mu\text{-}H)_2BC_8H_{14}]_2(PMe_3)$ (**7**)

	6, RX	**7**, DFT
Ru–B(1)	2.160(2)	2.179
Ru–B(2)	2.085(2)	2.122
Ru–P	2.2150(5)	2.230
Ru–H(1a)	1.63(2)	1.726
Ru–H(2a)	1.66(2)	1.726
Ru–H(1b)	1.60(2)	1.726
Ru–H(2b)	1.63(2)	1.726
B(1)–H(1a)	1.35(2)	1.404
B(1)–H(2a)	1.37(2)	1.404
B(2)–H(1b)	1.40(2)	1.414
B(2)–H(2b)	1.41(2)	1.414
B(2)–Ru–B(1)	147.68	150.2
B(1)–Ru–P	103.89(6)	101.5
B(2)–Ru–P	108.37(6)	108.3
P–Ru–H(1a)	94.0(8)	91.0
P–Ru–H(2a)	90.1(8)	91.0
P–Ru–H(1b)	90.2(8)	91.0
P–Ru–H(2b)	90.5(8)	91.0
H(1b)–Ru–H(2b)	77.8(11)	77.0
H(1a)–Ru–H(2a)	75.3(11)	77.9
H(1a)–B(1)–H(2a)	94.9(17	101.2
H(1b)–B(2)–H(2b)	92.7(13)	98.8

See Fig. 1 for labeling of the atoms. Distances are in angstrom and angles in degree.

ligand (1.38(4) and 1.28(3) Å) [13]. A ruthenium complex with a BBN inserted into the Ru–C bond of a metalated phosphine was reported with one B–H distance of 1.367(21) Å [15]. In our complex, small differences observed for the angles and the distances involving the two borons could indicate a disymmetry. An alternative formulation to the most plausible bis(dihydroborate) structure could be an intermediate structure with only one dihydroborate ligand, a hydrido and a σ-borane ligand. Such an hypothesis however seems unlikely and is not in agreement with NMR data showing at all temperatures only one signal for the four equivalents hydrogen.

DFT/B3LYP studies also favor the formation of the bis(dihydroborate) species. The model complex $Ru[(\mu\text{-}H)_2BC_8H_{14}]_2(PMe_3)$ (**7**) has been characterized on the singlet potential energy surface and has been shown to be a local minimum by vibrational frequency calculations. Optimized geometrical parameters and X-ray data are compared in Table 2. Our calculation confirms the overall structure found by X-ray diffraction. It is interesting to note that the difference observed for the P–Ru–B angles in the X-ray data is well reproduced by DFT calculations. A comparison of the B–H distances in **7** with free 9-BBN dimer (see below) allows an estimation of the degree of activation of the B–H bond during the coordination process. The lengthening is about 5% from the free ligand to **7** by DFT, and ca. 5–10% from the free ligand to **6** by X-ray. Wiberg indices obtained from an NBO analysis reflect an important delocalisation between the ruthenium, the two borons and the four bridging hydrogens, as seen for example from the following values: W(Ru–B1) 0.361, W(Ru–B2) 0.387, W(Ru–H1a) 0.274, W(Ru–H1b) 0.282, W(B1–H1a) 0.578, W(B2–H1b) 0.565. A more detailed NBO analysis does not seem to be appropriate, as it was impossible to obtain a Lewis structure representative of the coordination mode of two dihydroborate ligands on the same ruthenium atom.

Analysis of the crude ^1H- and ^{31}P-NMR spectra of the solution obtained after mixing **1** and 9-BBN dimer in toluene-d_8 shows apart from the formation of **6**, the presence of new signals attributed to the phosphine adduct $PCy_3\cdot HBC_8H_{14}$ (293 K: δ ^{31}P 10.2, 121.49 MHz; δ ^{11}B −14.7, 128.38 MHz;) (see Scheme 1) and less than 5% of $RuH[(\mu\text{-}H)_2\ BC_8H_{14}](H_2)(PCy_3)_2$ (**5**) (293 K, δ ^1H, −9.3 (vbr) 300 MHz, δ ^{31}P, 66.0 (br) 121.49 MHz, [11]).

The phosphine adduct was also characterized theoretically. We have optimized the 9-BBN dimer and the two adducts $PR_3\cdot HBC_8H_{14}$ (R = H, Me) at the DFT/B3LYP level. The corresponding geometries are depicted in Fig. 2 and optimized values of selected geometrical parameters as well as X-ray data for the 9-BBN dimer are reported in Table 3. The X-ray structure of 9-BBN was previously reported in 1973 [16], but we have now obtained new data at low temperature for better location of hydrogen atoms. The good agreement between the X-ray and the B3LYP-optimized geometries of the dimer testifies of the ability of the B3LYP hybrid functional to correctly describe two-electron three-center bonds. Moreover, an interesting comparison can be made with very recent X-ray and neutron data reported by Marder on the analogous dimesitylborane dimer $(HBMes)_2$ [17]. A B–H distance of 1.280(15) Å was determined by X-ray diffraction, whereas single crystal neutron diffraction at 20 K led to a value of 1.340(2) Å. In our case, the 9-BBN dimer is characterized by a B–H distance of 1.28(2) Å, as determined by X-ray, whereas the DFT/B3LYP calculation gives a value of 1.341 Å. This latter value thus correlates perfectly with the neutron determination on the dimesityl borane dimer. This comparison emphasises the importance of DFT calculations for a better estimation of the parameters concerning hydrogen atoms.

The decrease of the B–P bond length in the $PMe_3\cdot HBC_8H_{14}$ adduct compared to $PH_3\cdot HBC_8H_{14}$ is in agreement with the basicity of the PMe_3 ligand. The formation of the phosphine adduct corresponds to the following equation:

$$(HBC_8H_{14})_2 + 2PR_3 \rightarrow 2PR_3HBC_8H_{14} \quad (1)$$

The calculated ΔE energy difference associated with this equation is 12.3 kcal mol^{-1} in the case of PH_3 whereas a negative value of −11.1 kcal mol^{-1} is

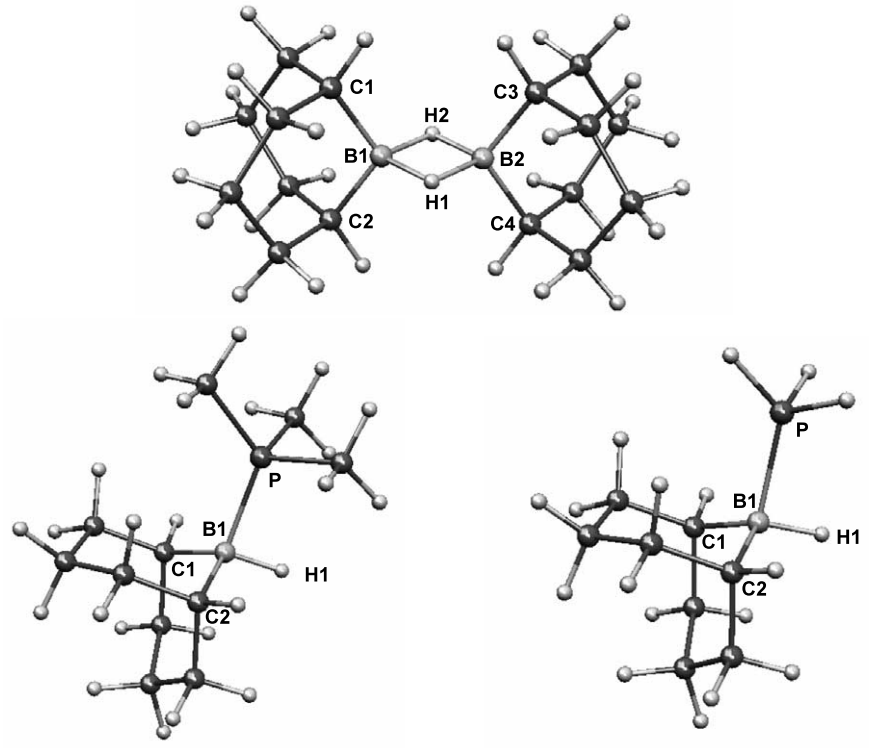

Fig. 2. The B3LYP-optimized structures of 9-BBN·($[HBC_8H_{14}]_2$) and the phosphine adducts $PH_3 \cdot HBC_8H_{14}$ and $PMe_3 \cdot HBC_8H_{14}$.

Table 3
X-ray data for 9-BBN and selected B3LYP-optimized geometrical parameters for 9-BBN and the phosphine adducts $PH_3 \cdot HBC_8H_{14}$ and $PMe_3 \cdot HBC_8H_{14}$

	9-BBN RX	9-BBN DFT	$PH_3 \cdot HBC_8H_{14}$ DFT	$PMe_3 \cdot HBC_8H_{14}$ DFT
B–H (av)	1.27(2)	1.341	1.232	1.240
B–C (av)	1.579(2)	1.598	1.625	1.634
B1–B2	1.804(3)	1.822	–	–
B1–P	–	–	2.040	1.995
H–B–H (av)	90(1)	94.4	–	–
B–H–B (av)	90(1)	85.6	–	–
C–B–C (av)	111.6(2)	111.2	108.5	107.3
C1–B1–B2	124.20(6)	124.4	–	–
H1–B1–P	–	–	93.4	93.3
P–B1–C1	–	–	111.5	115.0

See Fig. 2 for labeling of the atoms. Distances are in Å and angles in °.

obtained in the case of PMe_3. Standard enthalpies (ΔH°) and Gibbs free energies (ΔG°) at 298.15 K were obtained from vibrational frequency calculations. The ΔH° values for the PH_3 and PMe_3 adducts are 12.9 and -10.5 kcal mol^{-1}, respectively. They are not very different from the ΔE values. Taking into account the entropic factor leads to ΔG° values of 21.4 and 0.1 kcal mol^{-1}, respectively. These values indicate that the formation of the phosphine adduct cannot occur with PH_3 whereas it is likely with PMe_3, in better agreement with the experimental observation. This demonstrates that PH_3 cannot be used as a reasonable model of PCy_3 in our calculations.

3. Conclusion

In summary, we have isolated the first complex in which two 9-BBN ligands are coordinated to the same metal with a dihydroborate mode. This complex is obtained from the bis(dihydrogen) complex **1** in presence of an excess of 9-BBN, the driving force being the formation of the phosphine adduct $PCy_3 \cdot HBC_8H_{14}$. Our study demonstrates that in the field of borane activation, it is highly necessary to control the experimental conditions. Stoichiometric ratio and presence of water traces are in particular very important factors.

We have noted that a full NBO analysis of our system is not appropriate for such a delocalised electron density through four 3 center-2 electron B–H–Ru bonds. Moreover, as a result of possible interaction of the phosphine with the borane, we have shown that for borane activation by our ruthenium precursor, it is necessary for computational investigations to model the PCy_3 ligand by PMe_3. It is remarkable that in the case of

silane activation by the same precursor, PH_3 was a good model as the nature of the phosphine had little effect on the properties of the final product [14]. This is not true for borane activation. This should be probably the same for any other metal.

4. Experimental

4.1. General

All reactions were performed in an inert atmosphere glovebox or by using standard Schlenk techniques under argon. Solvents were dried and distilled according to standard procedures and degassed prior to use. All reagents were purchased from Aldrich except $RuCl_3 \cdot 3H_2O$ which came from Johnson Matthey Ltd. $RuH_2(H_2)_2(PCy_3)_2$ (**1**) was prepared according to published procedures [8]. All NMR solvents were dried using appropriate methods and degassed prior to use. NMR spectra were recorded on Bruker DPX 300 or AMX 400 spectrometers. ^{1}H-NMR chemical shifts are reported in ppm relative to residual ^{1}H signals in toluene-d_7 (δ 2.13) and ^{31}P-NMR in ppm downfield of an external 85% solution of phosphoric acid. ^{11}B-NMR chemical shifts are referenced to a $BF_3 \cdot Et_2O$ external standard solution.

4.2. Synthesis and characterization of *Ru[(μ-H)$_2$BC$_8$H$_{14}$]$_2$(PCy$_3$)* (*6*)

Toluene (3 ml) was added in the drybox to $RuH_2(H_2)_2(PCy_3)_2$ (**1**) (102.4 mg, 0.153 mmol) and 9-BBN dimer (114.2 mg, 0.468 mmol) in a Schlenk tube. Dihydrogen evolution was immediately observed followed by gradual dissolution of the solids within 2 h, producing an orange solution. The tube was then kept in the fridge at −35 °C. The resulting orange crystals were filtered off and dried under vacuum (yield 40%). Anal. Calc. for $C_{34}H_{65}B_2PRu$: C, 65.06; H, 10.46; Found C, 65.22; H, 10.39%. ^{1}H-NMR (toluene-d_8, 300.13 MHz) 293 K: δ 2–1.5 (m, 61H, C_8H_{14} and PCy_3), −12.43 (br, 4H, Ru–H_4); 243 K: −12.34 (d, 4H, Ru–H_4, $J_{H-P} = 9$ Hz). $T_{1\ min}$ (toluene-d_8, 300.13 MHz, 243 K) 95 ms. ^{31}P{^{1}H} NMR (toluene-d_8, 121.49 MHz) 293 K: 105.6 (s); 243 K: 105.5 (s). ^{31}P{^{1}H(PCy$_3$)} NMR (toluene-d_8, 161.98 MHz) 243 K: 104.9 (quintet, $J_{H-P} = 9$ Hz). ^{11}B{^{1}H} NMR (toluene-d_8, 96.29 MHz) 293 K: 58.8 (br).

4.3. NMR data for *RuH[(μ-H)$_2$BC$_8$H$_{14}$](H$_2$)(PCy$_3$)$_2$* (*5*)

^{1}H-NMR (toluene-d_8, 300.13 MHz) 293 K: δ −9.3 (vbr); 243 K: −4.9 (br, Ru-μ-H_2B), −11.48 (brt, RuH(H_2)). ^{31}P{^{1}H} NMR (toluene-d_8, 121.49 MHz) 293 K: 66.0 (br); 243 K: 65.8 (s).

4.4. Crystal data for *6*

Data were collected at low temperature ($T = 160$ K) on a Stoe Imaging Plate Diffraction System, equipped with an Oxford Cryosystems Cryostream Cooler Device and using a graphite-monochromated Mo–K_α radiation ($\lambda = 0.71073$ Å). The final unit cell parameters were obtained by least-squares refinement of a set of 8000 well measured reflections, and crystal decay was monitored by measuring 200 reflections by image. No significant fluctuation of the intensities was observed. A semi-empirical correction absorption was applied [18]. The structure was solved by direct methods using the program SIR92, [19] and refined by least-squares procedures on F^2 with SHELXL-97 [20] and WINGX [21]. The atomic scattering factors were taken from international tables for X-ray crystallography [22]. All hydrogen atoms were located on a difference Fourier map, but introduced and refined with a riding model. Hydride atoms were isotropically refined. All non-hydrogen atoms were anisotropically refined, a weighting scheme was used in the last cycles of refinement. Weights are calculated from the following formula: $w = 1/[\sigma^2(F_o^2) + (aP)^2 + bP]$ where $P = (F_o^2 + 2F_c^2)/3$. The molecule was drawn with the program ORTEP3 [23].

4.5. Computational details

DFT calculations were performed with the GAUSSIAN 98 series of programs [24] using the non-local hybrid functional denoted as B3LYP [25]. For ruthenium, the core electrons were represented by a relativistic small-core pseudopotential using the Durand–Barthelat method [26]. The 16 electrons corresponding to the 4s, 4p, 4d and 5s atomic orbitals were described by a (7s, 6p, 6d) primitive set of Gaussian functions contracted to (5s, 5p, 3d). Standard pseudopotentials developed in Toulouse were used to describe the atomic cores of all other non-hydrogen atoms (C, B and P) [27]. A double plus polarization valence basis set was employed for each atom (d-type function exponents were 0.80, 0.60 and 0.45, respectively). For hydrogen, a standard primitive (4s) basis contracted to (2s) was used. A p-type polarization function (exponent 0.9) was added for the hydrogen atoms directly bound to ruthenium. The geometry of the various critical points on the potential energy surface was fully optimized with the gradient method available in GAUSSIAN 98. Calculations of harmonic vibrational frequencies were performed to determine the nature of each critical point. See Ref. [28] for NBO analysis.

5. Supplementary material

Crystallographic data for the structural analysis have been deposited with the Cambridge Crystallographic Data Centre, CCDC no. 206648 and 206649 for **6** and 9-BBN dimer, respectively. Copies of this information may be obtained free of charge from The Director, CCDC, 12 Union Road, Cambridge CB2 1EZ, UK (Fax: +44-1223-336033; e-mail: deposit@ccdc.cam.ac.uk or www: http://www.ccdc.cam.ac.uk).

Acknowledgements

This work is supported by the CNRS. We thank the CINES (Montpellier, France) for a generous allocation of computer time.

References

[1] (a) H. Braunschweig, M. Colling, Coord. Chem. Rev. 223 (2001) 1;
(b) M.R. Smith, Prog. Inorg. Chem. 48 (1999) 505;
(c) G.J. Irvine, M.J.G. Lesley, T.B. Marder, N.C. Norman, C.R. Rice, E.G. Robins, W.R. Roper, G.R. Whittell, L.J. Wright, Chem. Rev. 98 (1998) 2685;
(d) H. Braunschweig, Angew. Chem. Int. Ed. 37 (1998) 1786;
(e) K. Burgess, M.J. Ohlmeyer, Chem. Rev. 91 (1991) 1179.

[2] G.J. Kubas, Metal Dihydrogen and σ-Bond Complexes, Kluwer Academic/Plenum Publishers, New York, 2001.

[3] (a) K.M. Waltz, J.F. Hartwig, J. Am. Chem. Soc. 122 (2000) 11358;
(b) H. Chen, S. Schlecht, T.C. Semple, J.F. Hartwig, Science 287 (2000) 1995;
(c) T. Ishiyama, J. Takagi, K. Ishida, N. Miyaura, N.R. Anastasi, J.F. Hartwig, J. Am. Chem. Soc. 124 (2002) 390.

[4] (a) J.-Y. Cho, M.K. Tse, D. Holmes, R.E. Maleczka, Jr., M.R. Smith, III, Science 295 (2002) 305;
(b) J.-Y. Cho, C.N. Iverson, Jr., M.R. Smith, III, J. Am. Chem. Soc. 122 (2000) 12868.

[5] (a) S. Shimada, A.S. Batsanov, J.A.K. Howard, T.B. Marder, Angew. Chem. Int. Ed. 40 (2001) 2168;
(b) R.B. Coapes, F.E.S. Souza, M.A. Fox, A.S. Batsanov, A.E. Goeta, D.S. Yufit, M.A. Leech, J.A.K. Howard, A.J. Scott, W. Clegg, T.B. Marder, J. Chem. Soc. Dalton Trans. (2001) 1201.

[6] M. Shimoi, S. Nagai, M. Ichikawa, Y. Kawano, K. Katoh, M. Uruichi, H. Ogino, J. Am. Chem. Soc. 121 (1999) 11704.

[7] (a) W.H. Lam, Z. Lin, Organometallics 22 (2003) 473;
(b) D. Liu, Z. Lin, Organometallics 21 (2002) 4750.

[8] (a) S. Sabo-Etienne, B. Chaudret, Coord. Chem. Rev. 178–180 (1998) 381;
(b) A.F. Borowski, B. Donnadieu, J.-C. Daran, S. Sabo-Etienne, B. Chaudret, Chem. Commun. (2000) 543;
(c) A.F. Borowski, B. Donnadieu, J.-C. Daran, S. Sabo-Etienne, B. Chaudret, Chem. Commun. (2000) 1697.

[9] V. Montiel-Palma, M. Lumbierres, B. Donnadieu, S. Sabo-Etienne, B. Chaudret, J. Am. Chem. Soc. 124 (2002) 5624.

[10] S. Lachaize, V. Montiel-Palma, B. Donnadieu, S. Sabo-Etienne, B. Chaudret, K. Essalah, J.C. Barthelat, to be published.

[11] A. Rodriguez, S. Sabo-Etienne, B. Chaudret, Anal. Quim. Int. Ed. (1996) 131.

[12] J.F. Hartwig, S.R. De Gala, J. Am. Chem. Soc. 117 (1994) 3661.

[13] A. Antinolo, F. Carrillo-Hermosilla, J. Fernandez-Baeza, S. Garcia-Yuste, A. Otero, A.M. Rodriguez, J. Sanchez-Prada, E. Villasenor, R. Gelabert, M. Moreno, J.M. Lluch, A. Lledos, Organometallics 19 (2000) 3654.

[14] (a) K. Hussein, C.J. Marsden, J.-C. Barthelat, V. Rodriguez, S. Conejero, S. Sabo-Etienne, B. Donnadieu, B. Chaudret, Chem. Commun. (1999) 1315;
(b) F. Delpech, S. Sabo-Etienne, J.C. Daran, B. Chaudret, K. Hussein, C.J. Marsden, J.-C. Barthelat, J. Am. Chem. Soc. 121 (1999) 6668;
(c) I. Atheaux, B. Donnadieu, V. Rodriguez, S. Sabo-Etienne, B. Chaudret, K. Hussein, J.-C. Barthelat, J. Am. Chem. Soc. 122 (2000) 5664.

[15] R.T. Baker, J.C. Calabrese, S.A. Westcott, T.B. Marder, J. Am. Chem. Soc. 117 (1995) 8777.

[16] B.J. Brauer, C. Krüger, Acta Crystallogr. B 29 (1973) 1684.

[17] T.B. Marder, personal communication. J. Organomet. Chem. (2003), in this issue.

[18] N. Walker, D. Stuart, DIFABS, Acta Crystallogr. Sect A, 39 (1983) 158.

[19] A. Altomare, G. Cascarano, G. Giacovazzo, A. Guagliardi, M.C. Burla, G. Polidori, M. Camalli, J. Appl. Cryst. 27 (1994) 435.

[20] G.M. Sheldrick, SHELXL-97—Program for Crystal Structure Analysis, Göttingen, Germany, 1998.

[21] L. Farrugia, WINGX-1.63 Integrated System of Windows Programs for the Solution, Refinement and Analysis of Single Crystal X-Ray Diffraction Data, J. Appl. Cryst. 32 (1999) 837.

[22] International Tables for X-ray crystallography, vol. IV, Kynoch press, Birmingham, England, 1974.

[23] L.J. Farrugia, ORTEP3 for Windows, J. Appl. Cryst. 30 (1997) 565.

[24] M.J. Frisch, G.W. Trucks, H.B. Schlegel, G.E. Scuseria, M.A. Robb, J.R. Cheeseman, V.G. Zakrzewski, J.A. Montgomery, Jr., R.E. Stratmann, J.C. Burant, S. Dapprich, J.M. Millam, A.D. Daniels, K.N. Kudin, M.C. Strain, O. Farkas, J. Tomasi, V. Barone, M. Cossi, R. Cammi, B. Mennucci, C. Pomelli, C. Adamo, S. Clifford, J. Ochterski, G.A. Petersson, P.Y. Ayala, Q. Cui, K. Morokuma, P. Salvador, J.J. Dannenberg, D.K. Malick, A.D. Rabuck, K. Raghavachari, J.B. Foresman, J. Cioslowski, J.V. Ortiz, A.G. Baboul, B.B. Stefanov, G. Liu, A. Liashenko, P. Piskorz, I. Komaromi, R. Gomperts, R.L. Martin, D.J. Fox, T. Keith, M.A. Al-Laham, C.Y. Peng, A. Nanayakkara, M. Challacombe, P.M.W. Gill, B. Johnson, W. Chen, M.W. Wong, J.L. Andres, C. Gonzalez, M. Head-Gordon, E.S. Replogle, J.A. Pople, Gaussian 98, Revision A.11, Gaussian, Inc., Pittsburgh PA, 2001.

[25] (a) A.D. Becke, J. Chem. Phys. 98 (1993) 5648;
(b) C. Lee, W. Yang, R.G. Parr, Phys. Rev. B 37 (1988) 785.

[26] P. Durand, J.-C. Barthelat, Theor. Chim. Acta 38 (1975) 283.

[27] Y. Bouteiller, C. Mijoule, M. Nizam, J.-C. Barthelat, J.-P. Daudey, M. Pélissier, B. Silvi, Mol. Phys. 65 (1988) 2664.

[28] A.E. Reed, L.A. Curtis, F. Weinhold, Chem. Rev. 88 (1988) 899.